Macromolecules

pubs.acs.org/Macromolecules Article

Single-Molecule Polypeptoid Stretching Reveals the Effects of Charge Sequence on Chain Conformation

Hoang P. Truong, Shawn Mengel, Beihang Yu, Rachel A. Segalman, and Omar A. Saleh*

Cite This: *Macromolecules* 2023, 56, 8558−8564 Read Online

ACCESS | Metrics & More | Article Recommendations | Supporting Information

ABSTRACT: Elucidating the effect of charge sequence on polyelectrolyte conformation is important to understanding many biophysical processes and advancing the design of sequence-defined polymeric materials. Such effects can be studied using polypeptoids, which permit the synthesis of polymer chains with precise monomer sequences. Here, we use single-molecule force experiments to explore the effect of charge spacing on polypeptoid conformation. We tested polypeptoid sequences composed of monomers that are either hydrophilic and uncharged or negatively charged. We find that the chain persistence length is insensitive to the net charge and ionic strength. With increasing solution ionic strength, we observe a good-to-theta transition in solvent quality with a theta point that scales with the charge spacing. Our results thus reveal a complex interplay between electrostatically driven excluded volume effects and charge-insensitive local conformational flexibility, which we posit is related to the location of charged groups on the side chains.

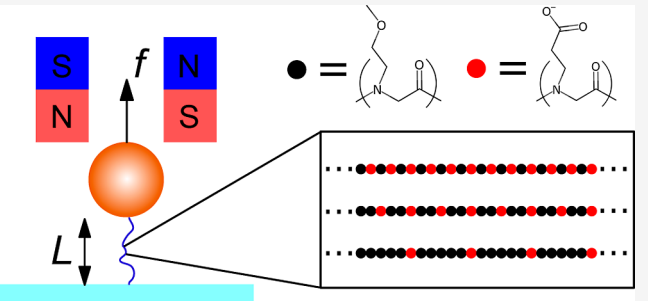

INTRODUCTION

Biopolymers, such as nucleic acids and proteins, encode their structure and functionality directly into their sequence. This has inspired the design of sequence-defined polymeric materials with engineered structural and functional complexity that approach those found in nature.[1−4] The rational *de novo* design of such materials requires a fundamental understanding of how the monomer sequence influences polymer conformation and structure. Specifically, electrostatic effects in polyelectrolytes have been broadly explored because they can drive structural formation and interactions with other molecules in the environment. Modulating a polyelectrolyte's charge sequence has been shown to significantly alter its conformational behavior[5−7] as well as its activity in many biophysical processes.[8,9] For example, complex coacervates formed by chains with longer charge blocks are found to have higher critical salt concentrations.[10,11]

Single-molecule force experiments provide a unique perspective on the behavior of polymers by using applied tension to probe chain structure and interactions over a broad range of length scales.[12] At intermediate to high forces (2−100 pN), the polymer chain is stretched to near its contour length, L_c. This regime disallows loop formation, allowing intrachain interactions only among neighboring monomers; the resulting elastic behavior thus gives insight into local polymer flexibility.[12] At very low forces (<1 pN), the polymer adopts "blob" configurations consisting of local self-avoiding random walks that are globally aligned with the applied force.[13] Prior single-molecule force experiments have exploited these low- and high-force elastic regimes to investigate the salt-dependent elasticity and structure of biological polyelectrolytes, such as single-stranded nucleic acids[14,15] and hyaluronic acid.[16] While these studies demonstrate the insights generated through single-molecule elasticity experiments, the polymers that were studied do not allow the modulation of key polyelectrolyte physical parameters, such as charge spacing.

Polypeptoids, or poly(*N*-substituted glycine)s, have emerged as a robust synthetic platform to explore the effect of sequence on chain conformation[17,18] because polypeptoids with specific sequences can be synthesized with high efficiency and precision.[19] Polypeptoids are analogous to peptides, having the same peptide backbone but with the side chains attached to the nitrogen instead of the α-carbon. This structure disallows the backbone−backbone hydrogen bonding prevalent in peptides, preventing secondary structure formation and enabling side chains to be the primary driver of intramolecular interactions.[20,21]

Here, we use single-molecule force experiments to test the effects of charge spacing on polypeptoid conformation. To isolate electrostatic effects, we test simple polypeptoid sequences that contain only two types of monomers, either negatively charged or hydrophilic and uncharged. For single-

Received: June 22, 2023
Revised: October 7, 2023
Accepted: October 16, 2023
Published: October 27, 2023

https://doi.org/10.1021/acs.macromol.3c01221
Macromolecules 2023, 56, 8558−8564

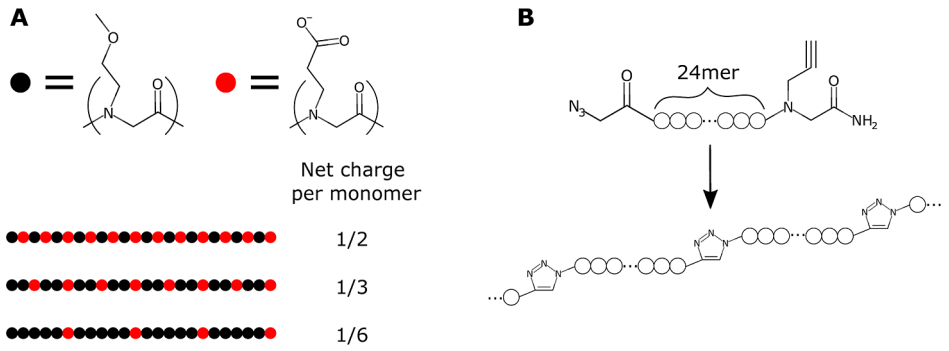

Figure 1. (A) Schematic of the polypeptoid sequences. Each sequence contains 2 types of monomers: hydrophilic and uncharged *N*-methoxyethyl (Nme) glycine (black circle), and negatively charged Nce glycine (red circle). (B) Attachment scheme to form long polypeptoids through end-to-end click reactions between 24mer polypeptoids.

molecule stretching experiments, we use end-to-end click reactions to create long polypeptoid chains. Our results show, surprisingly, that the polypeptoid persistence length does not vary with charge spacing or solution ionic strength. We further use low-force "Pincus blob" elasticity[13] to infer the solvent quality through the Flory exponent. We find a decrease in the Flory exponent with increasing solution ionic strength for all charge spacings, consistent with an electrostatically driven transition from good to theta solvent. Unlike the persistence length, the measured theta point is sensitive to the charge spacing of the polypeptoid sequence. We thus find two contrasting electrostatic effects, which we suggest can be reconciled by considering the location of the charges on the side chains of the polymer. Similarly complex electrostatic behaviors could occur in other polyelectrolytes with a similar pendant charge structure, such as peptides.

EXPERIMENTAL METHODS

Synthesis and Conjugation. Polypeptoids were synthesized on a Prelude synthesizer (Gyros Protein Technologies) using Rink amide resin (0.54 mmol/g, Novabiochem, San Diego, CA) using a protocol previously described.[21,22] The sequences contained 2-methoxyethylamine (Nme) and *β*-alanine *t*-butyl ester HCl *N*-carboxyethyl (Nce) submonomers, where the latter was free-based with aqueous potassium hydroxide and extracted with ethyl acetate. An alkyne group was included to the C-terminus of the sequence through the addition of the propargylamine submonomer in the first addition cycle. The N-terminus was acylated with bromoacetic acid, followed by a substitution with sodium azide, to form a terminal azide group. All other reagents and solvents were used as purchased without further modification or purification. The crude 24mers were purified with reverse phase preparative high-performance liquid chromatography, and the product was confirmed with MALDI (see the Supporting Information). A 12mer version of the 1/3 charge sequence was synthesized using the same protocol. The long polypeptoid click reaction was performed on the polypeptoids themselves (1 mM) with copper(II)-TBTA complex (prepared in 1:1 water/acetonitrile) (5 mM final) and ascorbic acid (5 mM final) in 200 *μ*L water under a N_2 gas. The excess catalysts and short polypeptoids were removed using an Amicon Ultra-0.5 centrifugal filter with a 100 kDa cutoff. The alkyne ends of the long polypeptoids (~120 *μ*g/mL) were capped with biotin-PEG3-azide (0.5 mM final) (Lumiprobe, Hunt Valley, MD), using a click reaction in water with copper(II)-TBTA complex (0.5 mM final) and ascorbic acid (0.5 mM final), followed by the same purification protocol above. We performed gel electrophoresis to characterize the presence of long polypeptoids,[23] finding a broad distribution of chain molecular weights that ranged up to about 500 kDa (see the Supporting Information).

Magnetic Tweezers Experiments. Long polypeptoids, at a concentration of ~6 *μ*g/mL, were attached to alkyne-coated, PEG-grafted glass surfaces (Microsurfaces, Inc.) in a solution of copper(II) sulfate (2.5 mM final) and ascorbic acid (2.5 mM final) in 1× phosphate-buffered saline with 0.1% Tween-20. The flow cell was washed with 10 mM tris buffer (pH 7.4) with 0.1% Tween-20. The biotin ends of the long polypeptoids were attached to 1 *μ*m diameter streptavidin-coated magnetic beads (Dynabeads MyOne Streptavidin C1, Invitrogen). The beads were incubated in the flow cell for 10 min, and then any unbound beads were washed away. The flow cell containing the attached long polypeptoids in tris buffer was placed on custom-built magnetic tweezers for single-molecule stretching experiments. Details on the instrument's setup and force calibration have been previously described.[24−26] Experiments were performed in 1−10 mM tris buffer (pH 7.5), 0−1000 mM NaCl, and 0.01−0.1% Tween-20. Only freshly made 1 mM tris buffer was used for experiments to prevent loss of buffering capacity and changes in pH. All experiments were performed at room temperature (20 °C).

RESULTS

Designing and Synthesizing Charge Sequences. We investigated three polypeptoid sequences, each with equally spaced charged monomers and a net charge per monomer, respectively, of 1/2, 1/3, and 1/6 (Figure 1A). The sequences thus varied in both net charge and charge spacing, which was accomplished by inserting varying numbers of neutral monomers between the charged carboxyl groups. Both types of monomers have the same number of *σ*-bonds along the length of the side chains, resulting in similar steric dimensions. The hydrophilic nature of the neutral side chains is expected to impart only excluded volume repulsion to the polymer. The spacing of charges along the backbone (0.6, 0.9, and 1.8 nm, respectively) is below the Debye screening length in low ionic strengths (~3 nm at 10 mM ionic strength), so intrachain electrostatic interactions were expected to be significant. We also synthesized a control polypeptoid sequence, consisting only of the neutral monomers, to investigate nonelectrostatic conformational behaviors.

After synthesizing individual 24mer polypeptoids, we quantified their charge state in solution through titration experiments (see Supporting Information). The measured pK_a values of the carboxylic acid (COOH) groups within the 1/2, 1/3, and 1/6 sequences were 5.51, 4.95, and 4.75, respectively. These values are similar to the reported pK_a of a glutamic acid protein residue (~4.25),[27] whose chemical structure is identical to the charged Nce peptoid side chain. Applying the Henderson-Hasselbalch equation at the experimental pH

https://doi.org/10.1021/acs.macromol.3c01221
Macromolecules 2023, 56, 8558−8564

of 7.4 indicates that the side chain groups in all sequences were ~99% deprotonated.

We used a polypeptoid synthesis scheme designed to generate long polymer chains suitable for single-molecule force experiments. Magnetic tweezers experiments require chains whose contour lengths are at least a few hundred nanometers, i.e., at least 1500 polypeptoid monomers, which far exceeds the practical limits of polypeptoid synthesis (well below 100mers).[28] To generate long chains, we incorporated azide and alkyne terminal functional groups on 24mer polypeptoids with the desired sequences, then used end-to-end click reactions (Figure 1B).[20,29] This attachment scheme imposes unidirectionality on the sequences, ensuring even charge spacing across the entire length of the long polypeptoids. We chose 24mers for the individual polypeptoid units as a compromise between synthesis efficiency and continuous polypeptoid bonding length.

Flexibility of Charged Polypeptoids. We analyzed the conformations of the various polypeptoid sequences through a single-molecule force–extension analysis using magnetic tweezers. For all sequences and solution conditions, the measured force–extension curves showed a low-force power-law elastic regime and a high-force regime with reduced compliance (Figure 2). Guided by theoretical considerations and analogous results on other flexible polymers,[12] we interpret the low-force regime as corresponding to the elasticity of a chain of tensile blobs, each of size k_BT/f, with looped, random-walk conformations within each blob.[13] At higher forces, tensile-blob elasticity disappears when all loops have been pulled out, i.e., at a crossover force where the tensile length roughly equals the persistence length, $k_BT/f_c \sim l_p$. At higher forces, $f > k_BT/l_p$, loops are prohibited, and thermal fluctuations only modestly misalign the statistical monomers from the direction of applied force; the lack of significant misalignment means there is little extension left to gain, and the compliance decreases as the chain approaches its contour length.

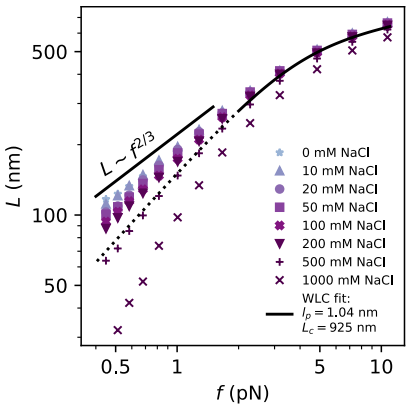

Figure 2. Force-extension data of a single polypeptoid molecule with a net charge per monomer of 1/2 in a solution of 1 mM tris, pH 7.4, and the indicated concentration of NaCl. The solid line is the WLC elastic curve using the best-fit contour length L_c and using the average l_p found from fitting to all curves measured in NaCl concentrations of less than 200 mM; fits were done only for forces above 2 pN. The low force extrapolation of the WLC model (dotted line) assumes ideal chain behavior; that this roughly matches the 500 mM NaCl data indicates this is a theta condition.

The elastic behavior of the polypeptoids at high force is accurately described by the Marko-Siggia wormlike-chain (WLC) model.[30] Particularly, we fit the force–extension data in this regime to an analytical solution of the WLC model derived by Bouchiat[31] with two fitting parameters: contour length, L_c, and persistence length, l_p (Figure 2). Given that the average l_p is ~1 nm, the crossover force is $f_c \sim 2$ pN. Since the WLC model does not account for swelling (self-avoidance) interactions, we fit the model only for forces above 2 pN. This method is self-consistent and the best-fit l_p values are not significantly sensitive to the cutoff choice. On each individual polypeptoid chain, several force-extension curves were acquired at different NaCl concentrations. Global WLC fitting was performed for each chain across all NaCl concentrations less than 200 mM, in which a single L_c was constrained for all such curves (since it is not expected to vary with salt), while l_p was fit individually for each curve. Goodness-of-fit metrics that account for the number of fit parameters indicate that this global method is modestly better than individual fitting of both L_c and l_p to each force-extension curve; further, the resulting l_p values do not significantly deviate between methods. Elastic measurements at 200 mM and higher ionic strengths indicate a small contraction (decrease of L_c) of the chains in those conditions; such curves are excluded from the global fits and instead fit individually. Such a contraction at high salt has been seen previously in other measurements[32] and has been attributed to salt-dependent water solvation effects. Measurements and fittings of various polypeptoid chains showed a range of contour lengths of 300–1000 nm, corresponding to chain sizes of 1000–3300 peptoid monomers, i.e., molecular weights of 125–410 kDa. Details of fitting parameters and residuals are discussed in the Supporting Information.

The persistence lengths of the polypeptoid sequences, as fit in the manner described above, are reported in Table 1. The measured values are similar to those observed in previous

Table 1. Persistence Lengths, in Nanometers, of Polypeptoids of Different Charge Fractions in Various Solution Ionic Strengths, I[a]

charge fraction	I = 8 mM	11 mM	21 mM	51 mM	101 mM	201 mM	501 mM	1001 mM
1/2	1.05 ± 0.03	1.08 ± 0.04	1.01 ± 0.04	1.03 ± 0.02	0.98 ± 0.04	1.00 ± 0.02	1.02 ± 0.02	1.08 ± 0.07
1/3	1.04 ± 0.02	1.10 ± 0.03	1.06 ± 0.06	1.10 ± 0.03	1.02 ± 0.02	1.03 ± 0.04	1.08 ± 0.01	
1/6	1.05 ± 0.02	1.08 ± 0.04	1.10 ± 0.02	1.05 ± 0.04	1.05 ± 0.03	1.09 ± 0.01	1.05 ± 0.02	
0	1.01 ± 0.03							
1/3 (12mer)	1.06 ± 0.04							

[a]Each value is the average of 3–19 different chains and the errors are the standard errors of the mean. I = 8 mM data was obtained in 10 mM tris pH 7.4. I > 8 mM data was obtained in 1 mM tris pH 7.4, with NaCl added to reach the indicated ionic strength. Charge fraction 0 corresponds to the control chain containing only neutral monomers. The last row indicates results on a chain formed from 12mers; all other rows correspond to 24mers.

https://doi.org/10.1021/acs.macromol.3c01221
Macromolecules 2023, 56, 8558–8564

studies, which range between 0.5 and 1 nm.[21,33,34] However, surprisingly, our results show that l_p is independent of the chain net charge. In addition, the l_p of each sequence is insensitive to salt concentration (Table 1). Further, in all conditions, the measured l_p values of the charged chains are not significantly different from that of the fully neutral control chain (Table 1).

The polypeptoid chains studied here have a heterogeneous backbone chemistry since the azide−alkyne click reactions form triazoles between every 24 polypeptoid monomers. Azide−alkyne cycloadditions have been widely explored in peptidomimetics, and the triazole product is comparable to a peptide bond in dimensionality, planarity, and polarity.[35,36] Nonetheless, it is possible that the triazole linkers have significantly different conformational properties that could affect our measurements of the chain flexibility. To examine this, we synthesized 12mer polypeptoids and assembled them into longer chains through the same click reactions, thus creating polymers with twice the density of triazoles. Elastic measurements showed that, with the same charge spacing, the 12mer polypeptoids do not show any significant change in l_p compared to the 24mer version (Table 1). This indicates that the measured elastic data are not significantly affected by the triazole linkers.

Polypeptoid Solubility and Theta Solvent. At low force, the observed power-law elasticity indicates that the polypeptoids can be described as a chain of tensile (Pincus) blobs, with solvent-quality-dependent random-walk behavior within each blob. Theory predicts that, in this regime, the extension scales with the force as $L \sim f^{1/\nu-1}$, where ν is the Flory exponent.[13] We find that the power law elasticity of polypeptoids is dependent on solution ionic strength (Figure 2), indicating that ν (and thus the solvent quality) varies with salt. At low ionic strength, the elastic exponent approaches 2/3, consistent with good solvent behavior (ν = 3/5). For all sequences, the elastic exponent increases with salt, passing through 1 between 100 and 1000 mM NaCl, indicating a theta point (i.e., effective ideal-chain behavior; ν = 0.5) at that salt. For the 1/2 charge sequence (Figure 2), the low force elasticity at 500 mM NaCl matches well with the extrapolation of the high-force WLC fits as the WLC model assumes ideal chain behavior;[37] this is further confirmation of the theta state at this solution condition. The Flory exponents found from the data, indicating the good-to-ideal solvent transition of each sequence, are shown in Figure 3A. Notably, the observed transition in solvent quality is similar to that of single-stranded DNA,[15] where the elastic exponent was also near 2/3 at lower ionic strengths and displayed an increase through 1 at high ionic strengths.

While all three sequences qualitatively exhibit the same decreasing trajectory of solvent quality with ionic strength, the quantitative details differ. Particularly, the theta salt concentration increases with decreasing charge spacing of the polypeptoid (Figure 3A). This indicates that the good solvent behavior stems, at least in part, from intrachain electrostatic repulsion. We interpret the theta behavior as resulting from screening of that repulsion by added salt until it is comparable to attractions within the chain (e.g., hydrophobic, van der Waals), with higher charge densities requiring more screening to reach the theta point. This suggests a unified view of the data might result through an analysis that accounts for the relative length scales of the charge density (charge spacing b) and the screening (Debye screening length κ^{-1}). We estimate b by taking the inter-residue spacing to be 0.3 nm, which is similar to the range of reported spacings of peptoid and peptide residues (0.3−0.4 nm).[38−41] Given that peptoids have a higher preference for the cis conformation than peptides,[42] and since the cis conformation shortens the residue spacing, we opted for a spacing on the low side of the range; however, our results are not significantly sensitive to this choice.

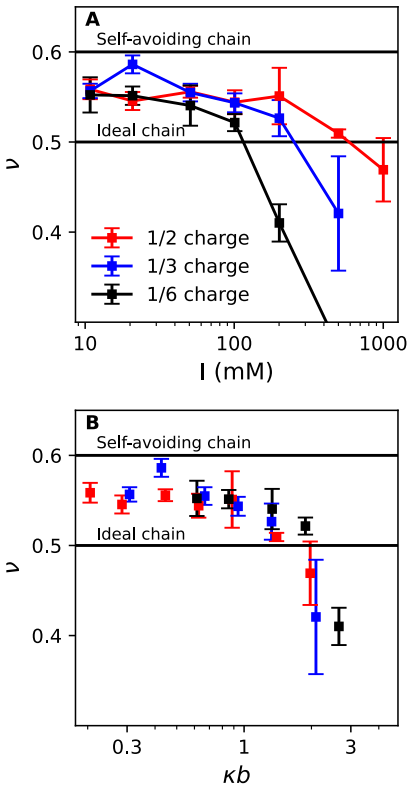

Figure 3. (A) Measured Flory exponents of the 3 charged polypeptoid sequences versus solution ionic strength. Each point represents 3−6 force-extension curves from separate polypeptoid molecules. Error bars indicate standard error of the mean. (B) Flory exponent data in (A) versus the unitless combination of Debye screening length, κ^{-1}, and charge spacing, b, of each sequence.

Figure 3B shows the Flory exponent plotted against the unitless ratio of the charge spacing and charge screening length, κb. We find that all three sequences collapse onto a single curve in this analysis, with the theta point corresponding roughly to $\kappa b \approx 1$. This indicates that when the Debye length becomes less than the length between charges, intrachain attractions begin to dominate, thus validating the idea that intermonomer repulsion is key to enabling good solvent behavior.

DISCUSSION

Our results indicate that the effect of charge spacing on a polypeptoid chain is somewhat nuanced, displaying opposing evidence regarding the significance of electrostatic effects. On the one hand, the charged groups show a clear effect in controlling solvent quality, with the collapse behavior depicted in Figure 3 specifically showing an effect of intrachain electrostatic screening. On the other hand, direct testing of conformational flexibility through high-force elasticity measurements (Table 1) shows no effects of either charge pattern or ionic strength on l_p. Importantly, control measurements confirm that the chain is indeed charged in the tested

https://doi.org/10.1021/acs.macromol.3c01221
Macromolecules 2023, 56, 8558−8564

conditions and that the chemistry used to synthesize long chains does not affect the measurements; these controls rule out certain explanations that could reconcile the observations.

It is possible that the two observations could be reconciled by considering the effect of force on the chain. While the estimate of Flory exponent relies on very low force ($f < 1$ pN) elasticity, the estimate of l_p relies on moderate-to-high force ($f > 2$ pN) elasticity. High force elasticity is generally a probe of shorter structural length scales in the polymer,[12] and prior simulation studies of polyelectrolytes found that the structure factors at short length scales are independent of chain charge density.[43,44] Further, a second potentially relevant influence is that the force itself can alter the short-range chain conformational flexibility,[45,46] possibly masking intrachain electrostatic effects. However, previous single-molecule studies on other polyelectrolytes, including single-stranded nucleic acids[14,15] and hyaluronic acid,[16] were able to elucidate electrostatic effects in this same force range. The difference between the present data and these prior works does not rely on the specific analysis scheme used here (WLC fitting), but it is more general: specifically, single-stranded nucleic acids and hyaluronic acids showed salt-induced changes in the shape of the force-extension curves that are absent here. We can thus generally conclude: (1) elastic measurements in the moderate force regime indeed probe length scales at which charge affects chain structure and therefore are capable of revealing electrostatic effects; and (2) any distortion of the chain structure by the applied force is not significant enough to conceal such electrostatic effects.

The relevance of these conclusions to the present measurements is strengthened by the comparison to hyaluronic acid[16] since the charge spacing of that chain ($b \approx 1$ nm) lies in the middle of the range of charge spacings of the polypeptoid sequences. Unlike the present data on polypeptoids, moderate-force elastic measurements of hyaluronic acid exhibited electrostatically dependent flexibility.[16] This indicates that our technique is capable of revealing electrostatic effects for a chain with a similar charge spacing, so it argues that some other aspect of the chain's chemical structure is likely responsible for the lack of observed electrostatic effects in the polypeptoids.

Further, a prior result on polypeptoids, using the same monomer chemistry as in this work, performed scattering measurements to conclude that the persistence length of a fully charged polypeptoid is significantly larger than that of a polypeptoid with alternating charges.[21] However, that result is not directly comparable to the present data as here we did not study a fully charged peptoid; further, the comparison is complicated by the differing techniques utilized, as well as the relatively large error bars shown in the prior work.[21]

We suggest that our observations on the opposing significance of electrostatic effects can be reconciled by considering the location of the charges in relation to the chain backbone. For single-stranded nucleic acids and hyaluronic acids, the charges are embedded in their backbones, maximizing the impact of electrostatics on the backbone flexibility. However, in the molecular structure of polypeptoids, the charged carboxyl groups are on side chains of moderate length, which could reduce electrostatic effects. When the side chain distance is significant, charge spacing can no longer be simply defined on the one-dimensional axis along the backbone; instead, the three-dimensional polymer configuration dictates the true distance between electrostatic groups. Notably, although the spacing of charged monomers along the backbone is 0.6 nm in the 1/2 charge sequence, the actual distance between charges could be as much as 0.9 nm, accounting for the side chain geometry. This increased distance would reduce the magnitude of repulsion between neighboring charged groups, thus minimizing the electrostatic effect on local chain flexibility (consistent with our results on l_p). On the other hand, the Flory exponent reflects monomer−monomer interactions on longer length scales and is less dependent on the location of the charged groups. This interpretation indicates why we observed electrostatic effects on solvent quality but not on local flexibility.

Prior works indeed show that the geometry of charged side chains in polyelectrolytes can influence their conformations[47,48] and secondary structure propensities.[49−53] For example, one prior work noted that, when charged groups are at a further distance from the backbone, there is a weakening of the intramolecular electrostatic repulsion.[53] However, the effect of the pendant charge specifically on the polyelectrolyte flexibility has not been extensively explored. To our knowledge, only the computational study of Ghelichi and Eikerling[47] has discussed the effect of charged side chain length on the persistence length. They found that the persistence length decreases with side chain length at lower charge fractions, yet the effect is opposite for a fully charged polyelectrolyte. However, the choice of polymer model and simulation conditions in that study prevents direct comparison with our results. Generally, future experimental works observing polyelectrolyte flexibility as a function of the side chain geometry would be highly valuable.

CONCLUSIONS

Through single-molecule stretching experiments, we tested the effect of charge spacing on the polypeptoid conformation. We find that local polypeptoid flexibility is insensitive to electrostatic effects, while the good-to-ideal solvent transition of all the polypeptoid sequences is dependent on their charge spacings. We posit that this electrostatic behavior, where only the polypeptoid solubility and not the flexibility is affected, could be due to the location of the charged groups on side chains that are separated by a moderate distance from the backbone.

Our hypothesis on the effect of side chain length on polymer flexibility could be useful to the investigation of other synthetic and biological polyelectrolytes and, indeed, the results of prior studies have hinted at an effect of side chains. For example, poly(acrylic acid), whose negative charges are ∼0.24 nm from its backbone, showed electrostatically dependent flexibility,[54] while polythiophenes, whose pendant imidazoles are ∼0.90 nm away from the backbone, were found to have no influence of charge fraction on their persistence lengths.[55] Further explorations of this hypothesis could involve other polymers with significant side chain lengths, such as poly[2-(dimethylamino)ethyl methacrylate] (∼0.63 nm) or random-coil polylysine (∼0.59 nm). A direct and systematic experimental investigation of the effect of side chain length on polyelectrolyte persistence length would be a particularly valuable study; one could approach this by designing and measuring a wide range of pendant charge distances on the same chemical backbone.

Generally, our results on the charge effects on polyelectrolyte flexibility and solvent quality are relevant to their use in a materials context, including in liquid−liquid phase separation

https://doi.org/10.1021/acs.macromol.3c01221
Macromolecules 2023, 56, 8558−8564

(LLPS) behavior.[10,56] Notably, the charge fractions of the polypeptoids in this study (1/2, 1/3, and 1/6) are similar to those of intrinsically disordered proteins that form biological coacervates (and in which the charges are also located on side chains);[57−59] thus, the electrostatic effects observed here will be useful for understanding their LLPS behavior.[60] Finally, this study demonstrates the utility of single-molecule force experiments for studying polymer sequence-conformation relationships. This experimental approach could be useful in the investigation of other sequence effects such as ampholyticity and hydrophobicity.

■ ASSOCIATED CONTENT

Supporting Information

The Supporting Information is available free of charge at https://pubs.acs.org/doi/10.1021/acs.macromol.3c01221.

MALDI spectra, SDS−PAGE image, titration plots, and detailed WLC fittings of polypeptoids (PDF)

■ AUTHOR INFORMATION

Corresponding Author

Omar A. Saleh − *Materials Department, University of California, Santa Barbara, California 93106, United States; Biomolecular Sciences and Engineering Program and Physics Department, University of California, Santa Barbara, California 93106, United States;* orcid.org/0000-0002-9197-4024; Email: saleh@ucsb.edu

Authors

Hoang P. Truong − *Materials Department, University of California, Santa Barbara, California 93106, United States;* orcid.org/0009-0003-0345-1923

Shawn Mengel − *Chemical Engineering Department, University of California, Santa Barbara, California 93106, United States*

Beihang Yu − *Chemical Engineering Department, University of California, Santa Barbara, California 93106, United States;* orcid.org/0000-0001-5060-0766

Rachel A. Segalman − *Materials Department and Chemical Engineering Department, University of California, Santa Barbara, California 93106, United States;* orcid.org/0000-0002-4292-5103

Complete contact information is available at: https://pubs.acs.org/10.1021/acs.macromol.3c01221

Notes

The authors declare no competing financial interest.

■ ACKNOWLEDGMENTS

The authors thank Prof. Javier Read de Alaniz for helpful discussions and his lab facility for assisting with several experiments. This work was supported by the National Science Foundation under award no. DMR-2005189. Some of the polypeptoid synthesis and characterization work was supported by the BioPACIFIC Materials Innovation Platform of the National Science Foundation under award no. DMR-1933487.

■ REFERENCES

(1) Nanjan, P.; Porel, M. Sequence-defined non-natural polymers: synthesis and applications. *Polym. Chem.* **2019**, *10*, 5406−5424.

(2) Meier, M. A.; Barner-Kowollik, C. A New Class of Materials: Sequence-Defined Macromolecules and Their Emerging Applications. *Adv. Mater.* **2019**, *31*, 1806027.

(3) Knight, A. S.; Zhou, E. Y.; Francis, M. B.; Zuckermann, R. N. Sequence programmable peptoid polymers for diverse materials applications. *Adv. Mater.* **2015**, *27*, 5665−5691.

(4) De Neve, J.; Haven, J. J.; Maes, L.; Junkers, T. Sequence-definition from controlled polymerization: the next generation of materials. *Polym. Chem.* **2018**, *9*, 4692−4705.

(5) Mao, A. H.; Crick, S. L.; Vitalis, A.; Chicoine, C. L.; Pappu, R. V. Net charge per residue modulates conformational ensembles of intrinsically disordered proteins. *Proc. Natl. Acad. Sci. U.S.A.* **2010**, *107*, 8183−8188.

(6) Müller-Späth, S.; Soranno, A.; Hirschfeld, V.; Hofmann, H.; Rüegger, S.; Reymond, L.; Nettels, D.; Schuler, B. Charge interactions can dominate the dimensions of intrinsically disordered proteins. *Proc. Natl. Acad. Sci. U.S.A.* **2010**, *107*, 14609−14614.

(7) Maity, H.; Baidya, L.; Reddy, G. Salt-induced transitions in the conformational ensembles of intrinsically disordered proteins. *J. Phys. Chem. B* **2022**, *126*, 5959−5971.

(8) Rubinstein, M.; Papoian, G. A. Polyelectrolytes in biology and soft matter. *Soft Matter* **2012**, *8*, 9265−9267.

(9) Schanze, K. S.; Shelton, A. H. Functional polyelectrolytes. *Langmuir* **2009**, *25*, 13698−13702.

(10) Chang, L.-W.; Lytle, T. K.; Radhakrishna, M.; Madinya, J. J.; Vélez, J.; Sing, C. E.; Perry, S. L. Sequence and entropy-based control of complex coacervates. *Nat. Commun.* **2017**, *8*, 1273−1278.

(11) Rumyantsev, A. M.; Jackson, N. E.; Yu, B.; Ting, J. M.; Chen, W.; Tirrell, M. V.; De Pablo, J. J. Controlling complex coacervation via random polyelectrolyte sequences. *ACS Macro Lett.* **2019**, *8*, 1296−1302.

(12) Saleh, O. A. Perspective: Single polymer mechanics across the force regimes. *J. Chem. Phys.* **2015**, *142*, 194902.

(13) Pincus, P. Excluded volume effects and stretched polymer chains. *Macromolecules* **1976**, *9*, 386−388.

(14) Jacobson, D. R.; McIntosh, D. B.; Stevens, M. J.; Rubinstein, M.; Saleh, O. A. Single-stranded nucleic acid elasticity arises from internal electrostatic tension. *Proc. Natl. Acad. Sci. U.S.A.* **2017**, *114*, 5095−5100.

(15) Saleh, O. A.; McIntosh, D.; Pincus, P.; Ribeck, N. Nonlinear low-force elasticity of single-stranded DNA molecules. *Phys. Rev. Lett.* **2009**, *102*, 068301.

(16) Berezney, J. P.; Saleh, O. A. Electrostatic effects on the conformation and elasticity of hyaluronic acid, a moderately flexible polyelectrolyte. *Macromolecules* **2017**, *50*, 1085−1089.

(17) Zuckermann, R. N. Peptoid origins. *Pept. Sci.* **2011**, *96*, 545−555.

(18) Sun, J.; Zuckermann, R. N. Peptoid polymers: a highly designable bioinspired material. *ACS Nano* **2013**, *7*, 4715−4732.

(19) Zuckermann, R. N.; Kerr, J. M.; Kent, S. B.; Moos, W. H. Efficient method for the preparation of peptoids [oligo (N-substituted glycines)] by submonomer solid-phase synthesis. *J. Am. Chem. Soc.* **1992**, *114*, 10646−10647.

(20) Murnen, H. K.; Khokhlov, A. R.; Khalatur, P. G.; Segalman, R. A.; Zuckermann, R. N. Impact of hydrophobic sequence patterning on the coil-to-globule transition of protein-like polymers. *Macromolecules* **2012**, *45*, 5229−5236.

(21) Murnen, H. K.; Rosales, A. M.; Dobrynin, A. V.; Zuckermann, R. N.; Segalman, R. A. Persistence length of polyelectrolytes with precisely located charges. *Soft Matter* **2013**, *9*, 90−98.

(22) Figliozzi, G. M.; Goldsmith, R.; Ng, S. C.; Banville, S. C.; Zuckermann, R. N. *Methods in Enzymology*; Elsevier, 1996; Vol. *267*, pp 437−447.

(23) Flood, D.; Proulx, C.; Robertson, E. J.; Battigelli, A.; Wang, S.; Schwartzberg, A. M.; Zuckermann, R. N. Improved chemical and mechanical stability of peptoid nanosheets by photo-crosslinking the hydrophobic core. *Chem. Commun.* **2016**, *52*, 4753−4756.

(24) Ribeck, N.; Saleh, O. A. Multiplexed single-molecule measurements with magnetic tweezers. *Rev. Sci. Instrum.* **2008**, *79*, 094301.

(25) Lansdorp, B. M.; Saleh, O. A. Power spectrum and Allan variance methods for calibrating single-molecule video-tracking instruments. *Rev. Sci. Instrum.* **2012**, *83*, 025115.
(26) Morgan, I. L.; Saleh, O. A. Tweezepy: A Python package for calibrating forces in single-molecule video-tracking experiments. *PLoS One* **2021**, *16*, No. e0262028.
(27) Lide, D. R. *CRC Handbook of Chemistry and Physics*; CRC Press, 2004; Vol. *85*.
(28) Davidson, E. C.; Rosales, A. M.; Patterson, A. L.; Russ, B.; Yu, B.; Zuckermann, R. N.; Segalman, R. A. Impact of helical chain shape in sequence-defined polymers on polypeptoid block copolymer self-assembly. *Macromolecules* **2018**, *51*, 2089−2098.
(29) Luo, K.; Yang, J.; Kopečková, P.; Kopeček, J. Biodegradable multiblock poly [N-(2-hydroxypropyl) methacrylamide] via reversible addition- fragmentation chain transfer polymerization and click chemistry. *Macromolecules* **2011**, *44*, 2481−2488.
(30) Marko, J. F.; Siggia, E. D. Stretching dna. *Macromolecules* **1995**, *28*, 8759−8770.
(31) Bouchiat, C.; Wang, M. D.; Allemand, J.-F.; Strick, T.; Block, S.; Croquette, V. Estimating the persistence length of a worm-like chain molecule from force-extension measurements. *Biophys. J.* **1999**, *76*, 409−413.
(32) McIntosh, D.; Saleh, O. A. Salt species-dependent electrostatic effects on ssDNA elasticity. *Macromolecules* **2011**, *44*, 2328−2333.
(33) Rosales, A. M.; Murnen, H. K.; Kline, S. R.; Zuckermann, R. N.; Segalman, R. A. Determination of the persistence length of helical and non-helical polypeptoids in solution. *Soft Matter* **2012**, *8*, 3673−3680.
(34) Yu, B.; Danielsen, S. P.; Yang, K.-C.; Ho, R.-M.; Walker, L. M.; Segalman, R. A. Insensitivity of sterically defined helical chain conformations to solvent quality in dilute solution. *ACS Macro Lett.* **2020**, *9*, 849−854.
(35) Angell, Y. L.; Burgess, K. Peptidomimetics via copper-catalyzed azide−alkyne cycloadditions. *Chem. Soc. Rev.* **2007**, *36*, 1674−1689.
(36) Holub, J. M.; Kirshenbaum, K. Tricks with clicks: modification of peptidomimetic oligomers via copper-catalyzed azide-alkyne [3+ 2] cycloaddition. *Chem. Soc. Rev.* **2010**, *39*, 1325−1337.
(37) McIntosh, D.; Ribeck, N.; Saleh, O. Detailed scaling analysis of low-force polyelectrolyte elasticity. *Phys. Rev. E* **2009**, *80*, 041803.
(38) Dietz, H.; Rief, M. Protein structure by mechanical triangulation. *Proc. Natl. Acad. Sci. U.S.A.* **2006**, *103*, 1244−1247.
(39) Erickson, H. P. Reversible unfolding of fibronectin type III and immunoglobulin domains provides the structural basis for stretch and elasticity of titin and fibronectin. *Proc. Natl. Acad. Sci. U.S.A.* **1994**, *91*, 10114−10118.
(40) Yang, G.; Cecconi, C.; Baase, W. A.; Vetter, I. R.; Breyer, W. A.; Haack, J. A.; Matthews, B. W.; Dahlquist, F. W.; Bustamante, C. Solid-state synthesis and mechanical unfolding of polymers of T4 lysozyme. *Proc. Natl. Acad. Sci. U.S.A.* **2000**, *97*, 139−144.
(41) Hudson, B. C.; Battigelli, A.; Connolly, M. D.; Edison, J.; Spencer, R. K.; Whitelam, S.; Zuckermann, R. N.; Paravastu, A. K. Evidence for cis amide bonds in peptoid nanosheets. *J. Phys. Chem. Lett.* **2018**, *9*, 2574−2578.
(42) Sui, Q.; Borchardt, D.; Rabenstein, D. L. Kinetics and equilibria of cis/trans isomerization of backbone amide bonds in peptoids. *J. Am. Chem. Soc.* **2007**, *129*, 12042−12048.
(43) Stevens, M. J.; Kremer, K. Form factor of salt-free linear polyelectrolytes. *Macromolecules* **1993**, *26*, 4717−4719.
(44) Stevens, M. J.; Kremer, K. The nature of flexible linear polyelectrolytes in salt free solution: A molecular dynamics study. *J. Chem. Phys.* **1995**, *103*, 1669−1690.
(45) Livadaru, L.; Netz, R.; Kreuzer, H. Stretching response of discrete semiflexible polymers. *Macromolecules* **2003**, *36*, 3732−3744.
(46) Dobrynin, A. V.; Carrillo, J.-M. Y.; Rubinstein, M. Chains are more flexible under tension. *Macromolecules* **2010**, *43*, 9181−9190.
(47) Ghelichi, M.; Eikerling, M. H. Conformational properties of comb-like polyelectrolytes: a coarse-grained MD study. *J. Phys. Chem. B* **2016**, *120*, 2859−2867.
(48) Tolmachev, D.; Lukasheva, N.; Mamistvalov, G.; Karttunen, M. Influence of Calcium Binding on Conformations and Motions of Anionic Polyamino Acids. Effect of Side Chain Length. *Polymers* **2020**, *12*, 1279.
(49) Pace, C. N.; Scholtz, J. M. A helix propensity scale based on experimental studies of peptides and proteins. *Biophys. J.* **1998**, *75*, 422−427.
(50) Kuo, H.-T.; Liu, S.-L.; Chiu, W.-C.; Fang, C.-J.; Chang, H.-C.; Wang, W.-R.; Yang, P.-A.; Li, J.-H.; Huang, S.-J.; Huang, S.-L.; Cheng, R. P. Effect of charged amino acid side chain length on lateral cross-strand interactions between carboxylate-and guanidinium-containing residues in a β-hairpin. *Amino Acids* **2015**, *47*, 885−898.
(51) Kuo, L.-H.; Li, J.-H.; Kuo, H.-T.; Hung, C.-Y.; Tsai, H.-Y.; Chiu, W.-C.; Wu, C.-H.; Wang, W.-R.; Yang, P.-A.; Yao, Y.-C.; Wong, T. W.; Huang, S.-J.; Huang, S.-L.; Cheng, R. P. Effect of charged amino acid side chain length at non-hydrogen bonded strand positions on β-hairpin stability. *Biochemistry* **2013**, *52*, 7785−7797.
(52) Meuzelaar, H.; Vreede, J.; Woutersen, S. Influence of Glu/Arg, Asp/Arg, and Glu/Lys Salt Bridges on α -Helical Stability and Folding Kinetics. *Biophys. J.* **2016**, *110*, 2328−2341.
(53) Lu, H.; Wang, J.; Bai, Y.; Lang, J. W.; Liu, S.; Lin, Y.; Cheng, J. Ionic polypeptides with unusual helical stability. *Nat. Commun.* **2011**, *2*, 206.
(54) Tricot, M. Comparison of experimental and theoretical persistence length of some polyelectrolytes at various ionic strengths. *Macromolecules* **1984**, *17*, 1698−1704.
(55) Danielsen, S. P.; Davidson, E. C.; Fredrickson, G. H.; Segalman, R. A. Absence of electrostatic rigidity in conjugated polyelectrolytes with pendant charges. *ACS Macro Lett.* **2019**, *8*, 1147−1152.
(56) Rumyantsev, A. M.; Jackson, N. E.; De Pablo, J. J. Polyelectrolyte complex coacervates: Recent developments and new frontiers. *Annu. Rev. Condens. Matter Phys.* **2021**, *12*, 155−176.
(57) Pak, C. W.; Kosno, M.; Holehouse, A. S.; Padrick, S. B.; Mittal, A.; Ali, R.; Yunus, A. A.; Liu, D. R.; Pappu, R. V.; Rosen, M. K. Sequence determinants of intracellular phase separation by complex coacervation of a disordered protein. *Mol. Cell* **2016**, *63*, 72−85.
(58) Zervoudis, N. A.; Obermeyer, A. C. The effects of protein charge patterning on complex coacervation. *Soft Matter* **2021**, *17*, 6637−6645.
(59) Nott, T. J.; Petsalaki, E.; Farber, P.; Jervis, D.; Fussner, E.; Plochowietz, A.; Craggs, T. D.; Bazett-Jones, D. P.; Pawson, T.; Forman-Kay, J. D.; Baldwin, A. J. Phase transition of a disordered nuage protein generates environmentally responsive membraneless organelles. *Mol. Cell* **2015**, *57*, 936−947.
(60) Uversky, V. N. Intrinsically disordered proteins in overcrowded milieu: Membrane-less organelles, phase separation, and intrinsic disorder. *Curr. Opin. Struct. Biol.* **2017**, *44*, 18−30.

https://doi.org/10.1021/acs.macromol.3c01221
Macromolecules 2023, 56, 8558−8564